Tectonophysics 482 (2010) 182–192

Contents lists available at ScienceDirect

Tectonophysics

journal homepage: www.elsevier.com/locate/tecto

Gravitational potential energy and regional stress and strain rate fields for continental plateaus: Examples from the central Andes and Colorado Plateau

Lucy M. Flesch [a], Corné Kreemer [b,*]

[a] Department of Earth and Atmospheric Sciences, Purdue University, West Lafayette, IN 47907, USA
[b] Nevada Bureau of Mines and Geology, and Seismological Laboratory, University of Nevada, Reno, NV 89557, USA

ARTICLE INFO

Article history:
Received 13 September 2008
Received in revised form 2 July 2009
Accepted 17 July 2009
Available online 24 July 2009

Keywords:
Tectonic stress
Plate boundary deformation
Gravitational potential energy
Lithospheric dynamics
Altiplano
Colorado Plateau

ABSTRACT

The commonly observed extension in areas of elevated and thickened crust is an expected consequence of having excess gravitational potential energy (GPE) compared to the low GPE of the surrounding crust. While this conceptual model is well founded, it is less clear how well GPE-related stress orientations compare quantitatively to observed stress and strain rate orientations and what any inconsistency tells us about the presence of other competing forces. We estimate the GPE distribution for the central Andes and the greater Colorado Plateau area using topography and crustal thickness variations, respectively, and compare the related stress fields with the World Stress Map as well as with a geodetic strain rate field (for the Colorado Plateau only). In both areas, deviatoric stresses associated with GPE variations alone cannot fully account for the observed deformation rate field. For the central Andes only a combination of deviatoric stresses associated with GPE and relative plate motions can account for the near N–S tensional stress observed in the Peruvian Andes and the margin–normal compressional stress along the eastern Cordillera and sub-Andean fold-and-thrust belt. The observed deformation field around the Colorado Plateau shows E–W extension, largely inconsistent with the deviatoric stresses associated with GPE variations except for the area east of the Rio Grande Rift. The NE–SW oriented stress observed on the southwestern Colorado Plateau is consistent with the orientations of tensional deviatoric stresses associated with GPE variations. We argue that this consistency could be haphazard; stress observations may not reflect the current state of stress due to inherited structure, or could result from the relative high strength of Colorado Plateau that allows for regional GPE variations (and possibly basal shear) to be more significant forces than far-field plate interactions. For the central Andes and Colorado Plateau, stresses associated with GPE variations have a strong influence on the total stress field, and can thus be used to calibrate the overall level of deviatoric stress acting within the lithosphere.

1. Introduction

The collapse of elevated and thickened crust and lithosphere (i.e., orogenic or gravitational collapse) is a natural consequence of the reduction of lateral differences in gravitational potential energy (GPE) acquired through the juxtaposition of crust/lithosphere of different density and/or thickness during the preceding mountain building phase (e.g., Bucher, 1956; van Bemmelen, 1954). The lateral GPE variations cause neighbouring lithospheric columns of high and low GPE to undergo tension and compression, respectively (e.g., Artyushkov, 1973; Fleitout and Froidevaux, 1982). Since the development of the concept, evidence for extension in orogenies (and the corollary shortening in the adjacent low lands) has frequently been attributed to GPE variations (e.g., Coney and Harms, 1984; Dalmayrac and Molnar, 1981; Dewey, 1988; Eva and Solarino, 1998; Hodges and Walker, 1992; Molnar and Lyon-Caen, 1988). This paradigm has, however, rarely been verified through a quantitative comparison of observed and modelled stress orientations. This lack of attention may be attributable to the fact that the origin of the stress field may also come from other processes such as basal shear tractions, related to lithosphere–mantle interaction, and boundary forces, related to relative plate motions. It is now recognized that a combination of deviatoric stresses associated with GPE and boundary forces can, to first order, explain the deformation field in the North American Cordillera (Flesch et al., 2000; Flesch et al., 2007; Humphreys and Coblentz, 2007), central Andes (Husson and Ricard, 2004; Liu et al., 2002), and Tibet (Flesch et al., 2001).

In light of this special volume, we apply the methodology presented by Flesch et al. (2001; 2007) to data from the World Stress Map (WSM; Heidbach et al. (2008a)) in order to reassess the origin of the stress fields for two arch-typical continental plateaus and their surroundings: the Colorado Plateau within the North American Cordillera of the southwestern United States, and the Altiplano within the surrounding central Andes. We hereby wish to revisit in more detail the comparison between observed stresses and deviatoric

* Corresponding author. Tel.: +1 775 682 8780; fax: +1 775 784 1709.
E-mail address: kreemer@unr.edu (C. Kreemer).

0040-1951/$ – see front matter © 2009 Elsevier B.V. All rights reserved.
doi:10.1016/j.tecto.2009.07.014

stresses predicted from GPE variations, relative plate motions, and the possible other forces needed to explain the observations. In addition, we wish to assess whether the effect of GPE variations can be seen using space-geodetic measurements of crustal deformation and how it may differ from stress observations. Such investigation will not be possible for the central Andes where the geodetic deformation field is dominated by elastic strain accumulation from coupling on the adjacent subduction mega-thrust (e.g., Bevis et al., 2001; Leffler et al., 1997; Norabuena et al., 1998), but is appropriate for the Colorado Plateau, which is located far from the main plate boundary in an area where measurements using the Global Positioning System (GPS) have rapidly accumulated over the last few years.

2. Deviatoric stresses associated with gravitational potential energy variations

In solving for the deviatoric stress field associated with GPE variations in the lithosphere we follow the method of Flesch et al. (2001, 2007) and treat the lithosphere as viscous continuum and use the thin sheet approximation (Bird and Piper, 1980; England and Houseman, 1986; England and Mckenzie, 1982) to solve for the vertically averaged deviatoric stress field. To directly quantify deviatoric stresses associated with GPE differences, we solve the vertically integrated force balance equations from the surface at $z=-h$, where h is the surface elevation, to the base of the lithosphere at a uniform depth $z=L$ (written in summation notation):

$$\frac{\partial}{\partial x_\beta}\left(\overline{\tau}_{\alpha\beta} + d_{\alpha\beta}\overline{\tau}_{\gamma\gamma}\right) = -\frac{\partial \overline{\sigma}_{zz}}{\partial x_\alpha} \tag{1}$$

where $\overline{\tau}_{ij}$ is the vertically averaged horizontal deviatoric stress tensor (i.e. xx, xy, yx, and yy components), and

$$\overline{\sigma}_{zz} = -\frac{1}{L}\int_{-h}^{L}\left[\int \rho(z')\mathrm{g}\mathrm{d}z'\right]\mathrm{d}z = -\frac{1}{L}\int_{-h}^{L}(L-z)\rho(z)\mathrm{g}\mathrm{d}z. \tag{2}$$

(See Flesch et al. (2007) for complete derivation.) The vertically averaged vertical stress defined in Eq. (2) is equivalent to $1/L$ times the gravitational potential energy per unit area defined with the reference level at the base of the lithosphere at depth L, and herein will be referred to as GPE. Eq. (1) is three equations with two unknowns, and Flesch et al. (2001) show that by imposing the constraint that the solution be the minimum deviatoric stress field solution a unique mathematical solution can be determined. Therefore, with a lateral estimate of GPE, we can directly solve Eq. (1) to determine a vertically averaged deviatoric stress field associated with body force distributions within the lithosphere (see Flesch et al. (2007) for details).

We estimate GPE values, $\overline{\sigma}_{zz}$, from topography and seismic data. For the western US we use the CRUST2.0 seismic crustal thickness data set (Bassin et al., 2000; Mooney et al., 1998) and Eq. (2) to calculate GPE estimates for each grid area. The mantle densities are modified to put each grid column in Airy isostatic balance. Because CRUST 2.0 does not provide the level of resolution we need for the Andes, we use the ETOPO5 data set there and assume constant crustal and mantle densities of 2750 kg/m^3 and 3300 kg/m^3, respectively. Assuming the lithosphere is in Airy isostatic balance, we calculate GPE for each grid area using Eq. (2). The magnitudes and distribution of GPE calibrate the magnitude of deviatoric stress acting in the lithosphere. The inherent uncertainty in calculating the stress field associated with GPE variations comes from the estimates of crustal thickness, assumed compensation, crustal density and mantle density.

Errors introduced variations in mantle density associated with lateral or isothermal temperature variations are small in comparison with the total magnitude of the GPE signal obtained form the crustal contribution. Furthermore, if the lithosphere is not fully in compensation, as has been proposed for the Andes, this would result in an overestimate of crustal thickness for each area. A reduction of crustal thickness would increase the amount of high density mantle that contributes to the integral for GPE, thus increasing the overall magnitude of the GPE estimates and associated deviatoric stresses. For a lithospheric column at 1.5 km elevation, decreasing the crustal thickness by 5 km produces a ~1% larger estimate of GPE. Furthermore, even though the magnitudes change slightly, the gradients of GPE do not. Thus, a GPE distribution calculated for a lithosphere not fully compensated would produce the same overall pattern of deviatoric stress.

3. Determination of stress field boundary conditions

We then follow the method of Flesch et al. (2007) and solve for a stress field boundary condition associated with plate interactions. We calculate stress field 3 normalized orthonormal basis functions for each boundary segment around the boundary of the grid using Eq. (1) and setting $\overline{\sigma}_{zz}=0$ (see Flesch et al. (2007) for details). For the Andes and the western US we divide the boundary into 47 and 49 segments, respectively. For each boundary segment we calculate the stress field response within the interior of the grid for corresponding to the three rotations of $w=(1,0,0)$, $(0,1,0)$, and $(0,0,1)$, yielding a total of 141 (47 segments$\times$3) and 147 (49 segments$\times$3) stress field basis functions. For the Andes case we also consider a single segment along the entire western boundary of the grid, and solve for 3 basis functions. The complete stress field boundary condition is the weighted linear sum of stress field basis functions, calculated around the boundary of the grid, which is added to our deviatoric stress field associated with GPE variations:

$$\tau = \tau_0 + \sum_{j=1}^{nseg}\sum_{i=1}^{3} a_{ij}\tau_{ij} \tag{3}$$

where τ_0 is the deviatoric stress tensor associated with GPE variations within the lithosphere that calibrates the magnitudes of the stress field basis functions, a_{ij} are the scaling factors for the stress field basis functions, and τ_{ij} are the stress field basis functions. The 141, 147, and 3 scaling factors, a_{ij}, (three for each boundary segment) are determined in an iterative least-squares inversion. The objective function we minimize is

$$\sum_{\text{areas}}\left\{T - \frac{(\dot{\varepsilon}\cdot\tau)}{E}\right\}DS. \tag{4}$$

where

$$E = \sqrt{\dot{\varepsilon}_{xx}^2 + \dot{\varepsilon}_{yy}^2 + \dot{\varepsilon}_{zz}^2 + \dot{\varepsilon}_{xy}^2 + \dot{\varepsilon}_{yx}^2} = \sqrt{2\dot{\varepsilon}_{xx}^2 + 2\dot{\varepsilon}_{xx}\dot{\varepsilon}_{yy} + 2\dot{\varepsilon}_{yy}^2 + 2\dot{\varepsilon}_{xy}^2},$$
$$T = \sqrt{\tau_{xx}^2 + \tau_{yy}^2 + \tau_{zz}^2 + \tau_{xy}^2 + \tau_{yx}^2} = \sqrt{2\tau_{xx}^2 + 2\tau_{xx}\tau_{yy} + 2\tau_{yy}^2 + 2\tau_{xy}^2},$$

$$\dot{\varepsilon}\cdot\tau = \{\dot{\varepsilon}_{xx}\tau_{xx} + \dot{\varepsilon}_{yy}\tau_{yy} + \dot{\varepsilon}_{zz}\tau_{zz} + \dot{\varepsilon}_{xy}\tau_{xy} + \dot{\varepsilon}_{yx}\tau_{yx}$$
$$= 2\dot{\varepsilon}_{xx}\tau_{xx} + \dot{\varepsilon}_{xx}\tau_{yy} + \dot{\varepsilon}_{yy}\tau_{xx} + 2\dot{\varepsilon}_{yy}\tau_{yy} + 2\dot{\varepsilon}_{xy}\tau_{xy}$$

DS is the grid area, $\dot{\varepsilon}_{ij}$ is the strain rate from the kinematic modelling or the smoothed stress field from the WSM and τ_{ij} is the total deviatoric stress tensor expressed in Eq. (5). This objective function is minimized when the orientations of principal axes of deviatoric stress are aligned with the orientations of principal axes of strain rates/stress observations and when the tectonic regime predicted by the deviatoric stress field (e.g., strike-slip, thrust, normal or a combination of these) matches the

observed tectonic regimes. We assess the goodness of fit between the modelled deviatoric stress field and observed stress indicators by calculating the average misfit:

$$M = \frac{1}{2}\left(1 - \frac{\dot{\varepsilon} \cdot \tau}{ET}\right). \quad (5)$$

4. Central Andes

The Andes were built as a consequence of the convergence of the Nazca and South American plates over the last 30 Myr (Dewey and Bird, 1970; Isacks, 1988). We define here the central Andes to be that part of the Cordillera located between 5° and 30°S (Fig. 1A), which encompasses the highest part of the Andes, the Altiplano plateau. There exists much evidence for extension in the central Andes and compression along its margins from seismicity (e.g., Assumpção and Araujo, 1993; Dalmayrac and Molnar, 1981; Déverchère et al., 1989; Doser, 1987; Suarez et al., 1983) and field studies (e.g., Allmendinger et al., 1989; McNulty and Farber, 2002; Mercier, 1981; Sébrier et al., 1985). The WSM contains the stress orientations from many of those observations, although there is a large number of data in the literature that is not included in the WSM (e.g., Allmendinger et al., 2005; Cladouhos et al., 1994; deUrreiztieta et al., 1996; Marrett et al., 1994; Siame et al., 2005). For the purpose of this study, we use the orientations maximum horizontal compressional stress ($S_{H\text{-}max}$) compiled in the WSM database to derive from these the principal horizontal directions of deviatoric stress tensor, i.e. tensional deviatoric stress orientations correspond to the orientations minimum horizontal compressional stress ($S_{H\text{-}min}$) and compressional deviatoric stress orientations equal the $S_{H\text{-}max}$ orientation (Fig. 1B). When multiple stress observations are present within the same model grid cells, we estimate an average (Fig. 1B).

The stress field in the central Andes (Fig. 1B) can be described as follows. The orientation of tensional deviatoric stress ($S_{H\text{-}min}$) in the high Andes is N–S, with most observations located along the Cordillera Blanca (in northern Peru), and in the northern limb of the Bolivian Orocline (southern Peru, and encompassing some of the northern Altiplano). N–S tensional stresses are also observed at low elevations in southern Peru. Almost no extension has been documented south of 18°S, including most of the Altiplano, with the notable exception of one observation of E–W tension along the coast of northern Chile. Compressional stresses perpendicular to the chain are found along most of the fold-and-thrust belt east of the Andes. Although the tensional deviatoric stress in Peru is now oriented N–S, it was markedly different before the Pleistocene, namely E–W (Mercier et al., 1992). Further south, in the Argentine Puna, the pre-Pleistocene stress field was WNW–ESE compressional (Cladouhos et al., 1994; Marrett et al., 1994). For Peru, Mercier et al. (1992) attributed the change in tectonic regime to time-variable coupling due to slab retreat, but it is now thought (Husson and Ricard, 2004; Liu et al., 2002) that the origin of the pre-Pleistocene E–W tensional stresses in Peru was a significant basal shear at a time when the convergence rate was higher (Pardo-Casas and Molnar, 1987; Somoza, 1998) and the Andes gained most of its elevation (e.g., Allmendinger et al., 1997; Isacks, 1988). It has been shown that basal tractions alone could be sufficient to raise the Andes (Wdowinski et al., 1989), and most recently Heidbach et al. (2008b) showed that the growth of the Andes would change the tectonic regime and rotate the stress orientations.

We use the ETOPO5 data set and Eq. (2) to estimate GPE variations and calculate the related principal axes of the vertically averaged horizontal deviatoric stress field (Fig. 2A). High values of GPE along the high Andes are accompanied by tensional deviatoric stresses up to ~20 MPa that are consistently orientated perpendicular to the chain. The magnitude of these deviatoric stresses is slightly lower than the preferred 25 MPa reported by Richardson and Coblentz (1994) based on a similar approach. Our model predicts tensional deviatoric stresses for all of the overriding plate up to the coastline. This result in itself is consistent with the observation margin–normal extension at low elevations for e.g. northern Chile (Delouis et al., 1998; González et al., 2003; Loveless et al., 2005), but inconsistent with earlier GPE-related stress field estimates that predicted extensional stresses to be contained to the area above 3000 m (Richardson and Coblentz, 1994). Deviatoric stresses are compressional in the oceanic lithosphere and

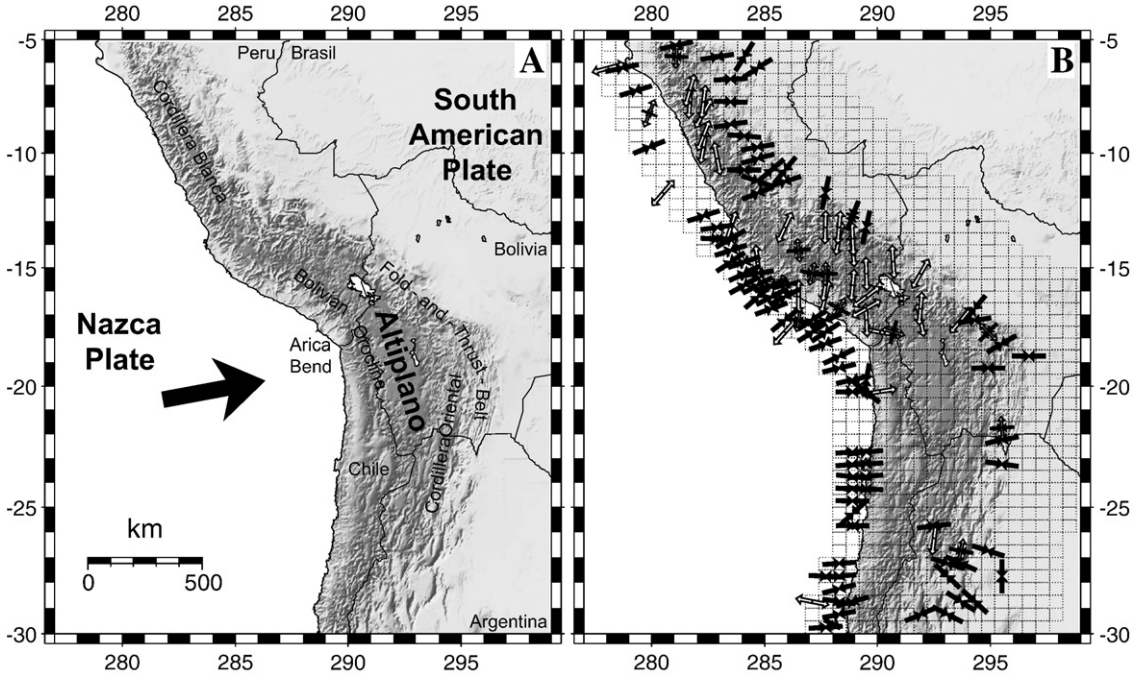

Fig. 1. (A) Regional setting of central Andes. Direction of Nazca–South America convergence is from Kreemer et al. (2003). (B) Dashed squares are model grid cells in which stress orientations, converted from WSM database (Heidbach et al., 2008a), are averaged. White and black arrows reflect extensional ($S_{H\text{-}min}$) and compressional ($S_{H\text{-}max}$) deviatoric stress orientations. Note that the principal stress orientations from the stress tensor (σ_{ij}) and the deviatoric stress tensor (τ_{ij}) are identical (Jaeger et al., 2007).

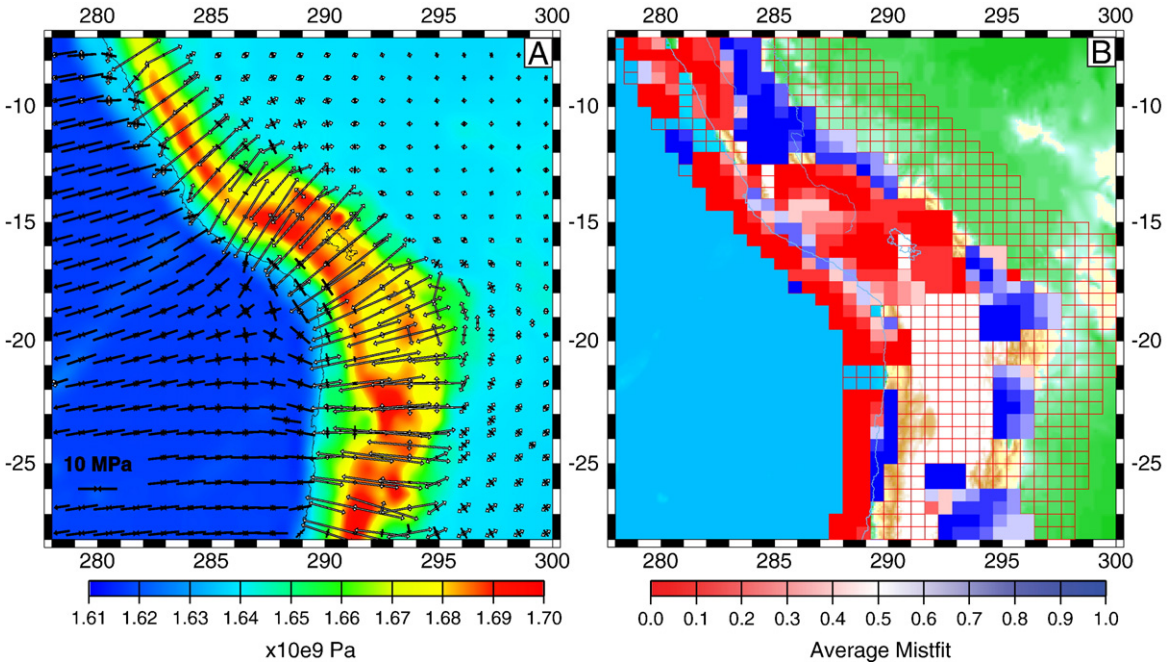

Fig. 2. (A) The vertically averaged deviatoric stresses field associated with GPE in the lithosphere. GPE estimates were determined using the ETOPO5 data set and assuming the lithosphere was in Airy isostatic balance, and are plotted as the background grid. White arrows represent the orientation of the tensional deviatoric stress and black arrows the orientation of the compressional deviatoric stress. (B) The average misfit between observed stress from the world stress map and the deviatoric stress field determined from GPE variations in A. The misfit function is given in Eq. (5).

are oriented roughly normal to the plate margin, except offshore from the Bolivian Orocline, near the Arica Bend, where E–W and NE–SW deviatoric compressional stresses are superimposed. Deviatoric stresses are slightly tensional along the fold-and-thrust belt and on the South American craton. The difference between the deviatoric stress field associated with GPE and the observed WSM stress field is estimated with misfit function in Eq. (5) (Fig. 2B). To increase the number of grid cells with WSM stress data with which to make the comparison, we smooth the observed stresses (Fig. 1B) one grid cell. We observe high misfits along the entire eastern Cordillera and fold-and-thrust belt, as well as for most of the Cordillera Blanca. The observed and estimated stress orientations in the high Andes are at significant angles with each other, except where they are both oriented NE–SW in the central Bolivian Orocline. The lack of overall agreement of the calculated deviatoric stress field with the stress observations argue for additional sources of stress.

To improve the model fit to the WSM stress observations we calculate a stress field boundary condition associated with plate interactions (Fig. 3A and B). We only use grid regions that contain smoothed stress observations when we invert for stress field boundary conditions. For 49 segment inversions, we find a stress field boundary condition of the order of ~15 MPa, which has a forces/unit length vector that is oriented very close to the Nazca–South America convergence direction (Fig. 3A). There are large deviatoric stresses along the eastern side of the grid, where no WSM stress observations are available. To demonstrate that these stresses are boundary effects due to lack of stress data we also invert for a single set of basis function segmented along the western boundary of the grid (Fig. 3B). The resultant stress field boundary condition is similar to the 49 segment inversion (consistent with the finding of Meijer et al. (1997) that the subduction related resistance force is constant along strike) and again produces a force/unit length vector in the direction of Nazca–South America convergence. However, this model does not contain the large stresses on the eastern boundary. The total deviatoric stress field (the sum of the stresses associated with GPE and plate interactions) (Fig. 3C and D) predicts deviatoric stresses along the subduction interface to be of the order of ~20–25 MPa, and the tensional deviatoric stresses in the Andes to be ~15 MPa in Peru and ~10 MPa further south. The total deviatoric stress field is broadly similar to the deviatoric stress field associated with GPE variations except that tensional deviatoric stresses in Peru are oriented more northward and that stresses east of the Andes are now more compressional and oriented normal to the chain. The total deviatoric stress field is nearly identical between the cases where we invert for 49 segments or a single segment to determine the plate boundary condition, with the 49 segment inversion producing a slightly lower misfit, 0.16, than the single segment inversion, 0.19 (Fig. 3E and F). This result suggests that a simple stress field boundary condition is sufficient to explain the WSM stress observations when added to the deviatoric stresses associated with GPE variations. Overall the total deviatoric stress field fits the observations significantly better than the deviatoric stress field due to GPE variations alone. However, it should be noted that the observed tensional deviatoric stresses in Peru are still oriented slightly more N–S than the predictions. Similar magnitude tensional deviatoric stresses are predicted along the central Andes south of 18°S, but are oriented E–W. Because almost no stress observations are present there, no misfit can be determined.

5. Colorado Plateau

The Colorado Plateau is a thick, elevated, and relatively undeformed physiographic province that has prevailed as an autonomous entity since the Permian. The prominent character of the Plateau is in part due to the fact that, unlike the Plateau's crust itself, the crust of adjacent provinces is severely extended: the Basin and Range Province to the south and west, and the Rio Grande Rift to the east (Fig. 4). Discussion on the exact mechanism that has caused and sustained the Plateau's elevation can be found elsewhere (McGetchin et al., 1980; Parsons and McCarthy, 1995; Thompson and Zoback, 1979). The current state of stress of the Plateau and its margins, as archived by the WSM and converted by us (Fig. 5A), can be described as follows. Within the Plateau and along its southwestern margin, stress orientations indicate a general pattern of NE–SW oriented tension that is consistently observed by the few determined

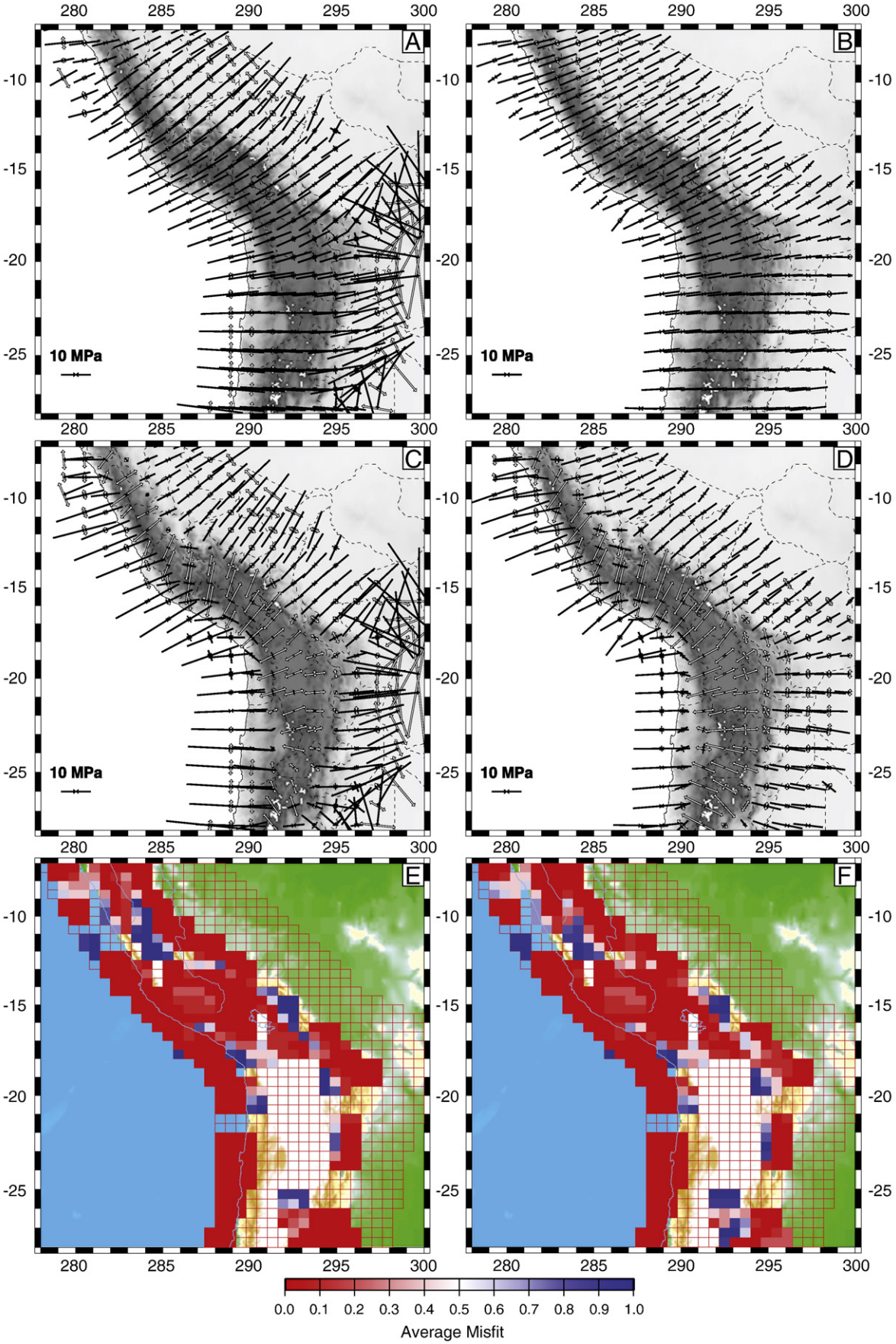
A
B
C
D
E
F
10 MPa
280
285
290
295
300
-10
-15
-20
-25
0.0 0.1 0.2 0.3 0.4 0.5 0.6 0.7 0.8 0.9 1.0
Average Misfit

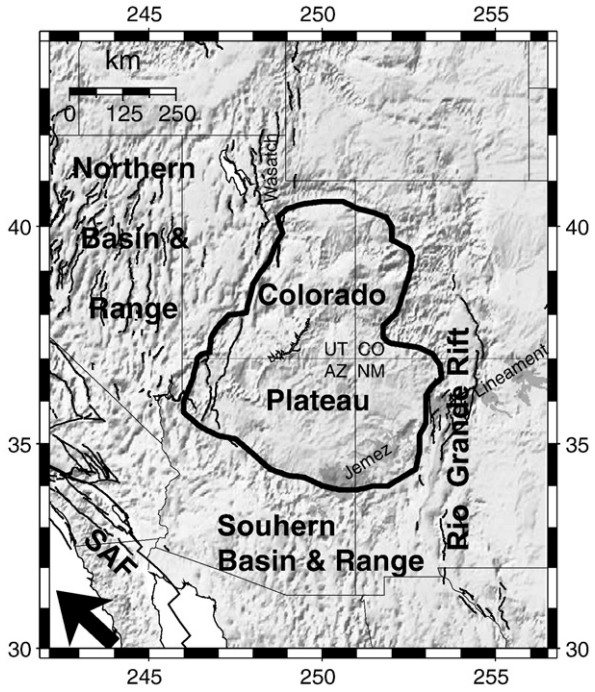

Fig. 4. Regional setting of Colorado Plateau, outlined by thick black line. Other black lines are Quaternary faults, and dark grey areas are the volcanic centers of the Jemez Lineament (from West et al. (2004)). SAF is San Andreas Fault system.

Rift and indicate E–W tension (Aldrich et al., 1986). The WSM catalogue does not contain any prominent stress signature associated with the southern Rio Grande Rift. Tensional stresses at the transition from the Colorado Plateau to the northern Basin and Range are WNW–ESE, similar to those in the Basin and Range (e.g., Patton and Zandt, 1991). Further north, along the Wasatch front, stress orientations are again more E–W.

In addition to the state of stress of the Colorado Plateau and its surroundings, another, and perhaps more direct, indication of the regional deformation field comes from a strain rate field as recorded by GPS measurements. We have processed data from all well-monumented continuous GPS sites that are part of various networks: EarthScope's Plate Boundary Observatory (PBO), Basin and Range Geodetic Network (BARGEN), Continuous Operating Reference stations (CORS) network, Southern California Integrated GPS (SCIGN) network, and the International GNSS Service (IGS) network. Horizontal velocities are determined for all sites with position time-series >2.5 years. Uncertainties in the velocities are estimated using the presence of colour and white-noise in the time-series. We then determine a continuous horizontal strain rate tensor field using a spline interpolation technique in which observed velocities are matched with associated model velocities in a least-squares sense (Beavan and Haines, 2001; Holt et al., 2000). The model strain rate field (Fig. 5B) is being characterized by having very low strain rates over most of the Colorado Plateau and areas to its north, east, and south. Yet, for all of the Colorado strain rates are indicating consistent E–W extension. East–west oriented extension is also observed along the transition of the Colorado Plateau and northern Basin and Range

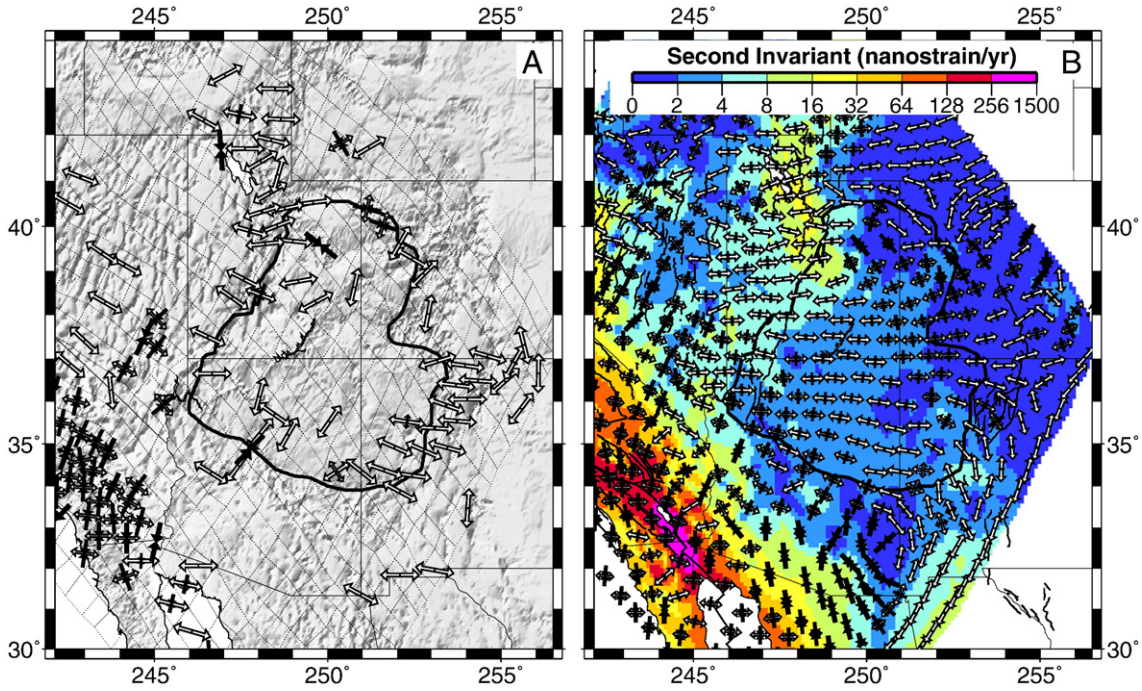

Fig. 5. Same as Fig. 1B but for Colorado Plateau. Arrow indicates direction of Pacific–North America plate motion (Kreemer et al., 2003). (B) Contours indicate second invariant of the modelled strain rate model inferred from GPS velocities. Vectors indicate the principal axes of the normalized strain rate tensor for each grid area (white is extension and black is contraction).

earthquake focal mechanisms (e.g., Brumbaugh, 2008b; Wong and Humphrey, 1989). Along its eastern margin most stress observations come from the volcanic Jemez Lineament and northern Rio Grande Province. Strain rates are 2–3 orders of magnitude higher along the San Andreas Fault system where strain rate tensors are predominantly reflecting shear.

Fig. 3. (A) The stress field boundary conditions associated with plate interactions determined using 49 boundary segments around the boundary of the grid. (B) Same as (A) only for a single segment stretching along the western boundary of the grid. (C) The vertically averaged total deviatoric stress field that is the sum of stresses associated with GPE variations (Fig. 2A) and the stress field boundary condition (A) for the case using 49 boundary segments. (D) Same as (C) only for the boundary condition case determined using a single segment around the boundary of the grid (B). (E) The misfit between the total vertically averaged deviatoric stress field determined using the 49 segment boundary condition and the observed stress from the world stress map. (F) Same as in (E) only for the total stress field case determined using the single segment stress field boundary condition. White arrows represent tensional deviatoric stress and black arrows compressional deviatoric stress. The misfit function is given in Eq. (5).

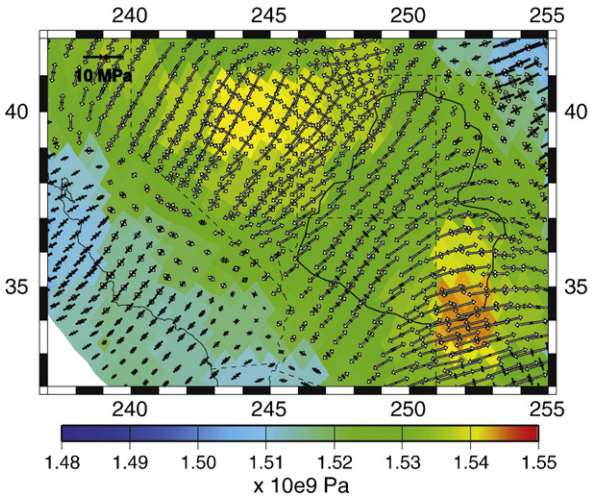

Fig. 6. The vertically averaged deviatoric stress field associated with GPE variations in the lithosphere. GPE estimates were determined using the CRUST2.0 data set and assuming the lithosphere was in Airy isostatic balance, and are plotted as the background grid. White arrows represent tensional deviatoric stress and black arrows compressional deviatoric stress.

The vertically averaged deviatoric stresses associated with GPE variations determined using the CRUST2.0 data set (Fig. 6) are very similar to that determined in Flesch et al. (2007) where a detailed discussion of this stress field is given for the entire plate boundary. Here we focus on the Colorado Plateau region in order to fully assess the sources of stress. Magnitudes of vertically averaged deviatoric stresses associated with GPE variations here range from 5–10 MPa and indicate NE–SW tension. We first compare the stresses associated with GPE variations with stress field indicators inferred from WSM (smoothed over 2 grid areas) and geodetic strain using the misfit function defined in Eq. (5) (Fig. 7). The misfit plots for the Colorado Plateau proper and the Rio Grande Rift show good agreement (misfit values ranging from 0–0.2) between deviatoric stresses associated with GPE variations and WSM stress indicators (Fig. 7A). In most other areas the misfit is larger (0.3–0.7) indicating that GPE variations alone cannot account for the stress observations and other driving forces are also acting. A similar conclusion can be drawn when using the GPS strain field instead of WSM stress indicators (Fig. 7B), except that the misfit is also poor for most of Colorado Plateau itself, especially its southwestern portion. That is, the GPE-related NE–SW oriented tension in the Plateau is not reflected in the GPS strain rate field. The area directly west of the Rio Grande Rift is the only region where the misfit appears consistently low.

To address these discrepancies, we solve for stress field boundary conditions associated with plate interactions (Flesch et al., 2007). We solve for two sets of stress field boundary conditions, either using the WSM (Fig. 8A) or geodetic strain rate model (Fig. 8B) as stress field indicators. Both sets of stress field boundary conditions are consistent with a shearing of the Pacific plate past the North American plate (Flesch et al., 2000; Flesch et al., 2007) with stress magnitudes ranging from 2–7 MPa, however, there are differences in the stress field boundary condition solutions. Inversions that use the WSM as stress field indicators tend to produce larger tensional deviatoric stresses in the southern region of the grid within Arizona, New Mexico and Colorado. For both (WSM and GPS) solutions the stress field boundary conditions in Arizona, New Mexico and Colorado tend to be smaller in magnitude than the stress field boundary conditions within northern region of the grid.

The vertically averaged total deviatoric stress field (Fig. 8C and D) (the sum of the stresses associated with GPE variations and stress field boundary conditions) is ENE–WSW tensional over the Colorado Plateau when we use either the WSM or geodetic strain as stress indicators (with the axes oriented slightly more E–W for the geodetic strain case). The similarity between the total deviatoric stress fields for the cases where we use WSM or geodetic strain as stress indicators is at a cost of having different total deviatoric stress fields closer to the Pacific plate. For both cases, large shear stresses are predicted in the Big Bend area, but deviatoric stresses along the southern San Andreas System are small and predominantly tension when using the WSM stress indicators, while they are larger and predominantly NNE–SSW compressional for the case where we aim to fit the geodetic strain. Misfits between the modelled vertically averaged total deviatoric stress field and the respective stress field indicators now produce misfits in the Colorado Plateau region with values ranging from 0–0.2 for both the WSM and GPS cases (Fig. 9). The low misfit in the case of using WSM stress indicators is about equal with the misfit between WSM stress indicators and GPE-derived stresses, indicating that in this case deviatoric stresses associated with relative plate motions mainly influence the deviatoric stress field further west. For the case of fitting geodetic strain rate orientations, the misfit across the

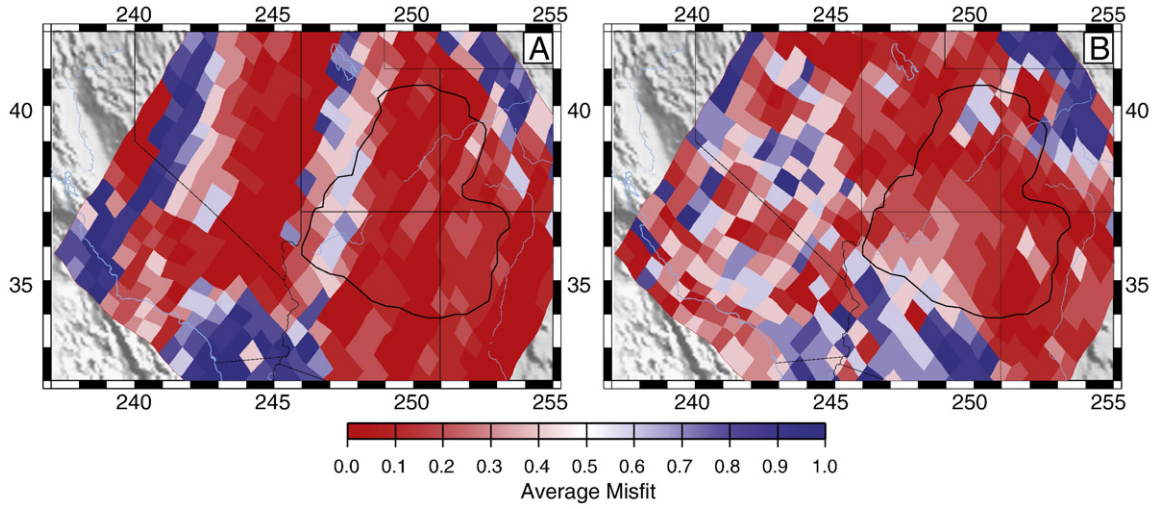

Fig. 7. (A) The average misfit between observed stress from the World Stress Map (Fig. 5A) and the vertically averaged deviatoric stress field determined from GPE variations (Fig. 6). (B) The average misfit between observed stress inferred using the strain rate field determined from GPS (Fig. 5B) and the vertically averaged deviatoric stress field determined from GPE variations (Fig. 6). The misfit function is given in Eq. (5).

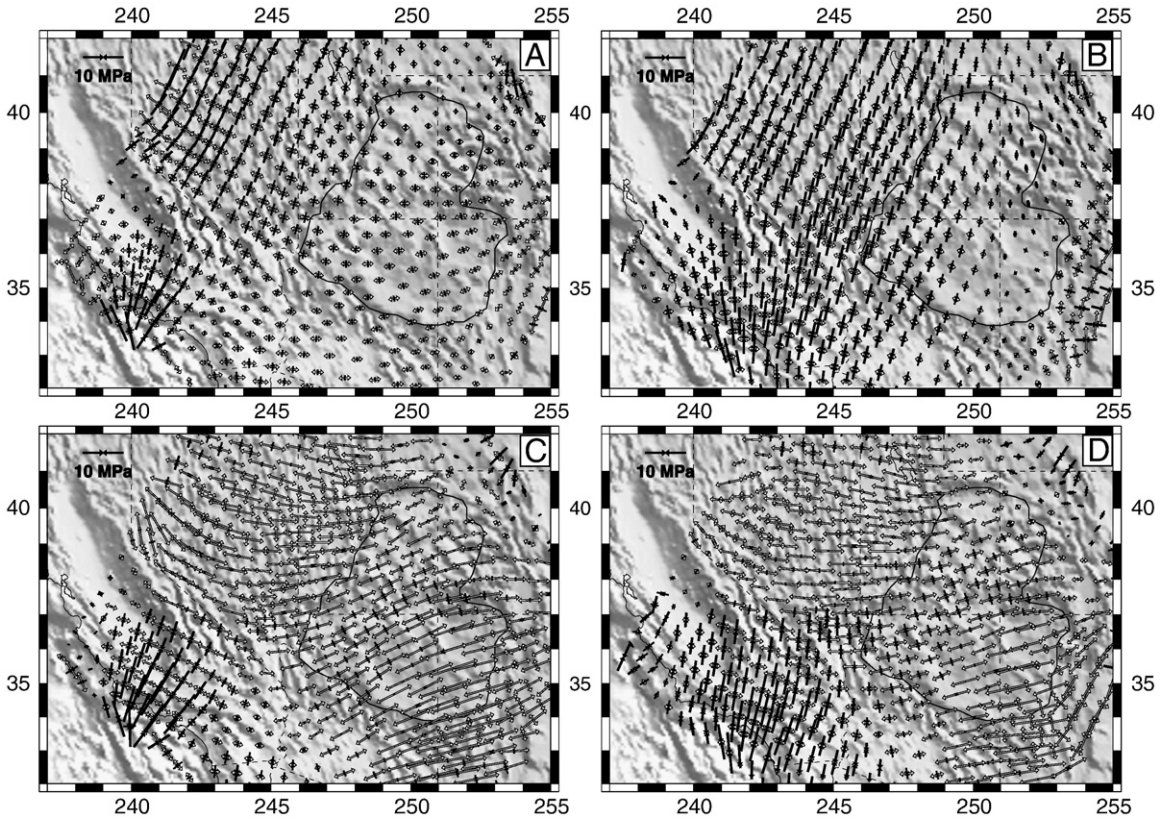

Fig. 8. (A) The stress field boundary condition that provides a best-fit to the stress field indicators inferred from the World Stress Map (Fig. 5A). (B) Same as in (A) only for stress indicators inferred from geodetic strain rates (Fig. 5B). (C) The total vertically averaged deviatoric stress field that is the sum of stresses associated with GPE (Fig. 6) and stress field boundary conditions (A) determined using the World Stress Map. (D) Same as (C) only for stress field boundary conditions determined using geodetic strain rates (B). White arrows represent tensional deviatoric stress and black arrows compressional deviatoric stress.

entire plate boundary reduced when the stress field boundary conditions are added to the deviatoric stresses associated with GPE variations.

6. Discussion and conclusions

For the central Andes we find that GPE variations alone cannot fully explain the observed stress observations. Additional deviatoric stresses due to Nazca–South America convergence are required, and as a result the stresses in the Peruvian Andes are more N–S oriented than predicted from GPE variations alone. We should note that required margin–normal deviatoric compressional stresses could also arise from basal tractions, but because we do not consider those, we may be estimating higher boundary forces to fit the data than would be the case if basal shear is significant. The relative role of basal tractions underneath the central Andes in explaining its (time-

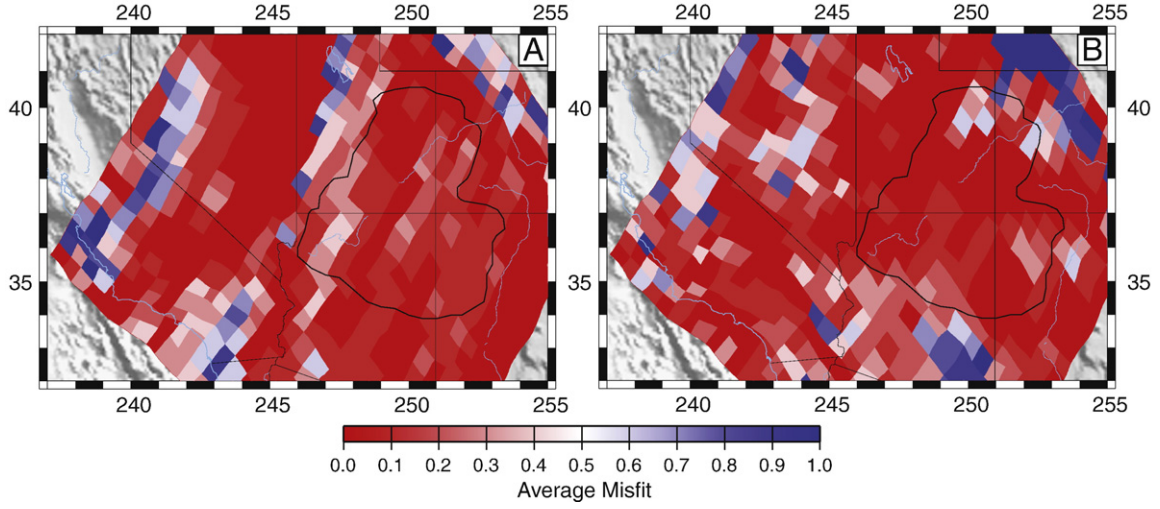

Fig. 9. (A) The average misfit between the total deviatoric stress field determined using the world stress map as stress field indicators (Fig. 8C) and stress indicators inferred from the World Stress Map (Fig. 4). (B) The average misfit between the total deviatoric stress field determined using the geodetic strain rates as stress field indicators (Fig. 8D) and stress indicators inferred from the geodetic strain rates (Fig. 5A). The misfit function is given in Eq. (5).

dependent) state of stress has been debated (e.g., Husson and Ricard, 2004; Liu et al., 2002; Meijer et al., 1997; Richardson and Coblentz, 1994; Wdowinski et al., 1989). Considering that our simple model (without invoking basal tractions) fits the stress orientations very well, we defer inclusion of basal tractions in our modelling. For now, we conclude that any total deviatoric stress coming from a combination of plate boundary forces and basal tractions is likely of similar magnitude as those presented here as coming from plate boundary forces alone.

Our result is different from that by Liu et al. (2002) who argued that deviatoric stresses resulting from GPE variations alone could explain the N–S extensional stresses in Peru. The absence of observed margin–normal extension in the Andes south of 18°S is likely due to the south-to-north change in the angle between the plate convergence direction and the plate margin. South of 18°S, deviatoric stresses associated with GPE variations are sub-parallel to the compressional deviatoric stresses from plate convergence and this could inhibit any extensional deformation there. The high GPE there may instead be reduced by horizontal spread of the lower crust (e.g., Bird, 1991; Rey et al., 2001). North of 18°S, compressional deviatoric stresses from plate boundary forces are oblique to tensional deviatoric stresses associated with GPE differences, allowing orogenic collapse there through faulting (and possibly also lower crustal flow). Husson and Ricard (2004) noted the role of obliquity as well to explain the extension in the northern limb of the Bolivian Orocline, and argued that, as this region keeps rotating counter-clockwise (as it has during the entire orogeny (e.g., Beck, 1987)), the gravitational collapse of this part of the Andes will accelerate.

Other explanations for the absence of observed WSM tensional stresses south of 18°S could come from variations in strength (i.e., the Andes south of 18°S being stronger than the Andes north of there) or due to slight variations in the actual stress field related to postseismic relaxation for which we do not account. However, we do not believe both explanations to be very plausible: we are not aware of any observed along-strike strength variation, and postseismic stresses in the overriding plate from past mega-thrust events are typically extensional (e.g., Khazaradze and Klotz, 2003; Wang et al., 2007), which should promote extension, not inhibit it. The only documented active extension in the overriding plate occurs through cracking and along normal faults in northern Chile, sometimes (but not necessarily) during or after subduction mega-thrust events (e.g., Delouis et al., 1998; González et al., 2003; Loveless et al., 2005). However, this extension is concentrated near the coast and does not contribute to the reduction of the high GPE of the high Andes.

As a corollary to having sub-parallel deviatoric tensional buoyancy forces and plate boundary compression south of 18°S, compressional deviatoric stresses in the fold-and-thrust belt are larger there than further north. The consequence of these large compressional deviatoric stresses is the presence of significant crustal shortening in the fold-and-thrust belt and eastern Cordillera, as observed by, e.g., Sheffels (1990), Baby et al. (1997), and Kley and Monaldi (1998), and argued by Liu et al. (2002) and Husson and Ricard (2004). Wdowinski and Bock (1994) argued that crustal shortening east of the Andes has increased over time as shortening migrated eastward due to increase in GPE during mountain building (causing a temporal shift from thick-skin to thin-skin tectonics). Our model also predicts compressional deviatoric stresses in the coastal areas of northern Chile and, most interestingly, suggests a component of margin parallel shortening. Margin-parallel shortening there has been evidenced to be active since the Miocene along E–W striking thrust faults (Allmendinger et al., 2005).

When using WSM stress indicators, our models suggest that GPE variations control the deviatoric stress field on the Colorado Plateau, but require additional deviatoric stresses from plate boundary interactions to explain the stress field further to the west. Although the stress field boundary conditions are only consistent in California and Nevada with expected shear and not in Arizona, New Mexico and Colorado, the above result confirms the importance of buoyancy forces in driving extension in the southwestern United States (e.g., Coney and Harms, 1984; Flesch et al., 2001; Humphreys and Coblentz, 2007; Jones et al., 1996; Liu, 2001). However, when using geodetic strain indicators, the role of GPE variations seem less significant than the WSM case, except for the southeastern Colorado Plateau where E–W extension appears to be controlled by GPE variations. Because the WSM stress and strain rate orientations are rather similar around most of the Colorado Plateau, the different results when using WSM or geodetic strain as stress indicators appears to come from the inconsistent data on the southwestern Colorado Plateau. There, geodetic strain rate orientations are oriented E–W, like elsewhere, but observed orientations of the minimum horizontal principal stress from the WSM are largely NE–SW. The deviatoric stress associated with GPE variations there are also oriented NE–SW, but does GPE control those stress orientations? It has long been known that the WSM minimum horizontal principal stress orientations in the southwestern United States were oriented NE–SW until ~20 Ma, when they started to rotate to more WNW–ESE direction coeval with the lengthening of the San Andreas Fault System (e.g., Bird, 2002; Zoback et al., 1981). The NE–SW oriented tensional stress field may have been driven by rapid rollback or delamination of the Farallon slab (Bird, 2002) and is in the same orientation as the mantle flow field (Becker et al., 2006; Moucha et al., 2008; Silver and Holt, 2002). It is possible that stress observations in the southwestern Colorado Plateau reflect the ancient stress regime. The high strength of the Colorado Plateau compared to its surroundings would inhibit the creation of new faults that would be more consistent with the present-day stress/strain field. The WSM stress observations come from focal mechanisms, which likely occur on pre-existing structures, and geologic indicators, which may come from the same structures. Instead of the WSM stress observations indicating the ancient stress regime, it is also possible that the relatively high strength of the Plateau makes it irresponsive to the far-field deviatoric stresses associated with relative plate motions and more susceptible to nearby forces such as GPE variations and/or basal drag. In fact, the horizontal deviatoric stresses due to basal tractions are tensional and oriented NW–SE underneath the Plateau (Flesch et al., 2007) and, when added to the NE–SW oriented deviatoric tensional stress due to GPE variations could yield the E–W extension observed in the geodetic strain rate field. It is thus possible that the effect of relative plate motions is less important than argued here and that basal tractions play a significant role. Future studies will bear this out. In any case, there is evidence that active E–W extensional tectonics along the margins of the Colorado Plateau is slowly migrating to the Plateau's central area (e.g., Aldrich and Laughlin, 1984; Brumbaugh, 2008a; Thompson and Zoback, 1979; Zoback and Zoback, 1980). This would suggest that the Colorado Plateau is slowing giving in to the prevailing E–W to ESE–WNW regional extension and that in the future the deformation field for all of the Colorado Plateau may be E–W extensional.

The consequence of the fact that deviatoric stresses associated with GPE variations fit WSM stress observations along the southwestern Plateau well is that in our modelling the calculated stress field boundary conditions are very small there. These small deviatoric stresses extend all the way to the San Andreas Fault system south of the Big Bend, and suggest a significant lateral change in the force that the Pacific plate exerts on the plate interior. Such a rapid lateral change in boundary condition is unphysical and not supported by other studies (Humphreys and Coblentz, 2007). We therefore conclude that using stress indicators to infer the relative role of GPE variations and boundary forces (and the spatial variation of the later) needs to be done with caution. Our preferred solution is therefore the one that uses the geodetic strain indicators. Our results from those models (i.e., combination of buoyancy and boundary forces are needed in almost the entire plate boundary to explain the deformation field) is consistent with earlier results that used

similar deformation indicators (Flesch et al., 2000, 2007). But, again, the possibility of there being a significant contribution from basal tractions cannot be ruled out by our current study.

Acknowledgments

C.K. acknowledges the financial support of the Task Force VII of the International Lithosphere Program (ILP). We thank R. Allmendinger, an anonymous reviewer, and the Guest Editor (O. Heidbach) for comments that helped to improve the manuscript, and W. Holt for his original encouragement to study the central Andes.

References

Aldrich, M.J., Chapin, C.E., Laughlin, A.W., 1986. Stress history and tectonic development of the Rio-Grande Rift, New-Mexico. Journal of Geophysical Research 91, 6199–6211.
Aldrich, M.J., Laughlin, A.W., 1984. A model for the tectonic development of the southeastern Colorado Plateau boundary. Journal of Geophysical Research 89 (Nb12), 207–218.
Allmendinger, R.W., Strecker, M., Eremchuck, J.E., Francis, P., 1989. Neotectonic deformation of the southern Puna Plateau, northwestern Argentina. Journal of South American Earth Sciences 2, 111–130.
Allmendinger, R.W., Jordan, T.E., Kay, S.M., Isacks, B.L., 1997. The evolution of the Altiplano–Puna plateau of the Central Andes. Annual Review of Earth and Planetary Sciences 25, 139–174.
Allmendinger, R.W., Gonzalez, G., Yu, J., Hoke, G., Isacks, B., 2005. Trench-parallel shortening in the Northern Chilean Forearc: tectonic and climatic implications. Geological Society of America Bulletin 117 (1–2), 89–104.
Artyushkov, E.V., 1973. Stresses in the lithosphere caused by crustal thickness inhomogeneities. Journal of Geophysical Research 78, 7675–7708.
Assumpção, M., Araujo, M., 1993. Effect of the Altiplano–Puna Plateau, South-America, on the regional intraplate stresses. Tectonophysics 221 (3–4), 475–496.
Baby, P., Rochat, P., Mascle, G., Herail, G., 1997. Neogene shortening contribution to crustal thickening in the back arc of the Central Andes. Geology 25, 883–886.
Bassin, C., Laske, G., Masters, G., 2000. The current limits of resolution for surface wave tomography in North America. Fall Meeting Suppl., EOS Trans., vol. 81. AGU, p. F897.
Beavan, J., Haines, J., 2001. Contemporary horizontal velocity and strain rate fields of the Pacific–Australian plate boundary zone through New Zealand. Journal of Geophysical Research 106, 741–770.
Beck, M.E., 1987. Tectonic rotations on the leading-edge of South America — the Bolivian Orocline revisited. Geology 15, 806–808.
Becker, T.W., Schulte-Pelkum, V., Blackman, D.K., Kellogg, J.B., O Connell, R.J., 2006. Mantle flow under the western United States from shear wave splitting. Earth and Planetary Science Letters 247, 235–251.
Bevis, M., et al., 2001. On the strength of interplate coupling and the rate of back arc convergence in the central Andes: an analysis of the interseismic velocity field. Geochemistry Geophysics Geosystems 2 2001GC000198.
Bird, P., 1991. Lateral extrusion of lower crust from under high topography, in the isostatic limit. Journal of Geophysical Research 96, 10275–10286.
Bird, P., 2002. Stress direction history of the western United States and Mexico since 85 Ma. Tectonics 21, 1014. doi:10.1029/2001TC001319.
Bird, P., Piper, K., 1980. Plane-stress finite-element models of tectonic flow in southern California. Physics of the Earth and Planetary Interiors 21, 158–175.
Brumbaugh, D.S., 2008a. Seismicity and active faulting of the Kanab–Fredonia area of the southern Colorado Plateau. Journal of Geophysical Research 113, B055309. doi:10.1029/2007JB005278.
Brumbaugh, D.S., 2008b. Seismicity and tectonics of the Blue Ridge area of the Mogollon Plateau. Arizona Bulletin of the Seismological Society of America, vol. 98, pp. 1527–1534.
Bucher, W.H., 1956. Role of gravity in orogenesis. Geological Society of America Bulletin 67, 1295–1318.
Cladouhos, T.T., Allmendinger, R.W., Coira, B., Farrar, E., 1994. Late Cenozoic deformation in the central Andes — FAULT kinematics from the northern Puna, northwestern Argentina and southwestern Bolivia. Journal of South American Earth Sciences 7 (2), 209–228.
Coney, P.J., Harms, T.A., 1984. Cordilleran metamorphic core complexes — Cenozoic extensional relics of Mesozoic compression. Geology 12, 550–554.
Dalmayrac, B., Molnar, P., 1981. Parallel thrust and normal faulting in Peru and constraints on the state of stress. Earth and Planetary Science Letters 55, 473–481.
Delouis, B., Philip, H., Dorbath, L., Cisternas, A., 1998. Recent crustal deformation in the Antofagasta region (northern Chile) and the subduction process. Geophysical Journal International 132, 302–338.
deUrreiztieta, M., Gapais, D., LeCorre, C., Cobbold, P.R., Rossello, E., 1996. Cenozoic dextral transpression and basin development at the southern edge of the Puna Plateau, northwestern Argentina. Tectonophysics 254 (1–2), 17–39.
Déverchère, J., Dorbath, C., Dorbath, L., 1989. Extension related to a high topography — Results from a microearthquake survey in the Andes of Peru and tectonic implications. Geophysical Journal International 98, 281–292.
Dewey, J.F., 1988. Extensional collapse of orogens. Tectonics 7, 1123–1139.
Dewey, J.F., Bird, J.M., 1970. Mountain belts and new global tectonics. Journal of Geophysical Research 75, 2625–2647.
Doser, D.I., 1987. The Ancash, Peru, earthquake of 1946 November 10 — evidence for low-angle normal faulting in the high Andes of northern Peru. Geophysical Journal of the Royal Astronomical Society 91, 57–71.
England, P., Houseman, G., 1986. Finite strain calculations of continental deformation. 2. Comparison with the India–Asia collision zone. Journal of Geophysical Research 91, 3664–3676.
England, P., Mckenzie, D., 1982. A thin viscous sheet model for continental deformation. Geophysical Journal of the Royal Astronomical Society 70, 295–321.
Eva, E., Solarino, S., 1998. Variations of stress directions in the western Alpine arc. Geophysical Journal International 135, 438–448.
Fleitout, L., Froidevaux, C., 1982. Tectonics and topography for a lithosphere containing density heterogeneities. Tectonics 1, 21–56.
Flesch, L.M., Holt, W.E., Haines, A.J., Shen-Tu, B., 2000. Dynamics of the Pacific–North American plate boundary in the western United States. Science 287, 834–836.
Flesch, L.M., Haines, A.J., Holt, W.E., 2001. Dynamics of the India–Eurasia collision zone. Journal of Geophysical Research 106, 16435–16460.
Flesch, L.M., Holt, W.E., Haines, A.J., Wen, L.X., Shen-Tu, B., 2007. The dynamics of western North America: stress magnitudes and the relative role of gravitational potential energy, plate interaction at the boundary and basal tractions. Geophysical Journal International 169, 866–896.
González, G., Cembrano, J., Carrizo, D., Macci, A., Schneider, H., 2003. The link between forearc tectonics and Pliocene–Quaternary deformation of the Coastal Cordillera, northern Chile. Journal of South American Earth Sciences 16 (5), 321–342.
Heidbach, O., Tingay, M., Barth, A., Reinecker, J., Kurfeß, D. and Müller, B., 2008a. The World Stress Map database release 2008. doi:10.1594/GFZ.WSM.Rel2008.
Heidbach, O., Iaffaldano, G., Bunge, H.P., 2008b. Topography growth drives stress rotations in the central Andes: observations and models. Geophysical Research Letters 35, L08301. doi:10.1029/2007GL032782.
Hodges, K.V., Walker, J.D., 1992. Extension in the Cretaceous Sevier Orogen, North-American Cordillera. Geological Society of America Bulletin 104, 560–569.
Holt, W.E., Shen-Tu, B., Haines, J., Jackson, J., 2000. On the determination of self-consistent strain rate fields within zones of distributed deformation. In: Richards, M.A., Gordon, R.G., van der Hilst, R.D. (Eds.), The History and Dynamics of Global Plate Motions. Geophysical Monograph. AGU, Washington, D.C., pp. 113–141.
Humphreys, E.D., Coblentz, D.D., 2007. North America dynamics and western U.S. tectonics. Reviews of Geophysics 45, RG3001. doi:10.1029/2005RG000181.
Husson, L., Ricard, Y., 2004. Stress balance above subduction: application to the Andes. Earth and Planetary Science Letters 222, 1037–1050.
Isacks, B.L., 1988. Uplift of the central Andean Plateau and bending of the Bolivian Orocline. Journal of Geophysical Research 93, 3211–3231.
Jaeger, J.C., Cook, N.G.W., Zimmermann, R.W., 2007. Fundamentals of Rock Mechanics, 4th ed. Blackwell Publishing, Oxford.
Jones, C.H., Unruh, J.R., Sonder, L.J., 1996. The role of gravitational potential energy in active deformation in the southwestern United States. Nature 381, 37–41.
Khazaradze, G., Klotz, J., 2003. Short- and long-term effects of GPS measured crustal deformation rates along the south central Andes. Journal of Geophysical Research 108, 2289. doi:10.1029/2002JB001879.
Kley, J., Monaldi, C.R., 1998. Tectonic shortening and crustal thickness in the Central Andes: how good is the correlation? Geology 26, 723–726.
Kreemer, C., Holt, W.E., Haines, A.J., 2003. An integrated global model of present-day plate motions and plate boundary deformation. Geophysical Journal International 154, 8–34.
Leffler, L., et al., 1997. Constraints on present-day shortening rate across the central eastern Andes from GPS data. Geophysical Research Letters 24, 1031–1034.
Liu, M., 2001. Cenozoic extension and magmatism in the North American Cordillera: the role of gravitational collapse. Tectonophysics 342, 407–433.
Liu, M., Yang, Y., Stein, S., Klosko, E., 2002. Crustal shortening and extension in the central Andes: insights from a viscoelastic model. In: Stein, S., Freymueller, J.T. (Eds.), Plate Boundary Zones. American Geophysical Union, Washington, D.C., pp. 325–339.
Loveless, J.P., et al., 2005. Pervasive cracking of the northern Chilean Coastal Cordillera: new evidence for forearc extension. Geology 33, 973–976.
Marrett, R.A., Allmendinger, R.W., Alonso, R.N., Drake, R.E., 1994. Late Cenozoic tectonic evolution of the Puna Plateau and adjacent foreland, northwestern Argentine Andes. Journal of South American Earth Sciences 7 (2), 179–207.
McGetchin, T.R., Burke, K.C., Thompson, G.A., Young, R.A., 1980. Mode and mechanisms of plateau uplifts. In: Balley, A., Bender, P.L., McGetchin, T.R., Walcott, R.I. (Eds.), Dynamics of Plate Interiors. American Geophysical Union, Washington D.C., pp. 99–110.
McNulty, B., Farber, D., 2002. Active detachment faulting above the Peruvian flat slab. Geology 30, 567–570.
Meijer, P.T., Govers, R., Wortel, M.J.R., 1997. Forces controlling the present-day state of stress in the Andes. Earth and Planetary Science Letters 148 (1–2), 157–170.
Mercier, J.L., 1981. Extensional–compressional tectonics associated with the Aegean arc: comparison with the Andean Cordillera of south Peru–north Bolivia. Philosophical Transactions of the Royal Society London, series A 300, 337–355.
Mercier, J.L., et al., 1992. Changes in the tectonic regime above a subduction zone of Andean type — the Andes of Peru and Bolivia during the Pliocene–Pleistocene. Journal of Geophysical Research 97, 11945–11982.
Molnar, P., Lyon-Caen, H., 1988. Some simple physical aspects of the supprt, structure, and evolution of mountain belts. Geological Society of America Special Paper 218, 179–207.
Mooney, W.D., Laske, G., Masters, T.G., 1998. CRUST 5.1: a global crustal model at 5 degrees × 5 degrees. Journal of Geophysical Research 103, 727–747.
Moucha, R., et al., 2008. Mantle convection and the recent evolution of the Colorado Plateau and the Rio Grande Rift valley. Geology 36 (6), 439–442.
Norabuena, E., et al., 1998. Space geodetic observations of Nazca–South America convergence across the central Andes. Science 279, 358–362.

Pardo-Casas, F., Molnar, P., 1987. Relative motion of the Nazca (Farallon) and South American plates since late Cretaceaous time. Tectonics 6, 233–248.
Parsons, T., McCarthy, J., 1995. The active southwest margin of the Colorado Plateau — uplift of mantle origin. Geological Society of America Bulletin 107, 139–147.
Patton, H.J., Zandt, G., 1991. Seismic moment tensors of western United States earthquakes and implications for the tectonic stress-field. Journal of Geophysical Research 96, 18,245–18,259.
Rey, P., Vanderhaeghe, O., Teyssier, C., 2001. Gravitational collapse of the continental crust: definition, regimes and modes. Tectonophysics 342, 435–449.
Richardson, R.M., Coblentz, D.D., 1994. Stress modeling in the Andes — constraints on the South American intraplate stress magnitudes. Journal of Geophysical Research 99, 22015–22025.
Sébrier, M., Mercier, J.L., Mégard, F., Laubacher, G., Carey-Gailhardis, E., 1985. Quaternary normal and reverse faulting and the state of stress in the central Andes of south Peru. Tectonics 4, 739–780.
Sheffels, B.M., 1990. Lower bound on the amount of crustal shortening in the central Bolivian Andes. Geology 18, 812–815.
Siame, L.L., Bellier, O., Sebrier, M., Araujo, M., 2005. Deformation partitioning in flat subduction setting: case of the Andean foreland of western Argentina (28 degrees S-33 degrees S). Tectonics 24, TC5003. doi:10.1029/2005TC001787.
Silver, P.G., Holt, W.E., 2002. The mantle flow field beneath western North America. Science 295, 1054–1057.
Somoza, R., 1998. Updated Nazca (Farallon)-South America relative motions during the last 40 Myr. Journal of South American Earth Sciences 11, 211–215.
Suarez, G., Molnar, P., Burchfiel, B.C., 1983. Seismicity, fault plane solutions, depth of faulting, and active tectonics of the Andes of Peru, Ecuador, and southern Colombia. Journal of Geophysical Research 88, 403–428.
Thompson, G.A., Zoback, M.L., 1979. Regional geophysics of the Colorado Plateau. Tectonophysics 61, 149–181.
van Bemmelen, R.W., 1954. Mountain Building. Martinus Nijhoff, The Hague. 177 pp.
Wang, K., et al., 2007. Crustal motion in the zone of the 1960 Chile earthquake: detangling earthquake-cycle deformation and forearc-sliver translation. Geochemistry Geophysics Geosystems 8, Q10010. doi:10.1029/2007GC001721.
Wdowinski, S., Bock, Y., 1994. The evolution of deformation and topography of high elevated plateaus. 2. Application to the central Andes. Journal of Geophysical Research 99, 7121–7130.
Wdowinski, S., Oconnell, R.J., England, P., 1989. A continuum model of continental deformation above subduction zones — application to the Andes and the Aegean. Journal of Geophysical Research 94, 10,331–10,346.
West, M., et al., 2004. Crust and upper mantle shear wave structure of the southwest United States: implications for rifting and support for high elevation. Journal of Geophysical Research 109, B03309. doi:10.1029/2003JB002575(B3).
Wong, I.G., Humphrey, J.R., 1989. Contemporary seismicity, faulting, and the state of stress in the Colorado Plateau. Geological Society of America Bulletin 101, 1127–1146.
Zoback, M.L., Zoback, M., 1980. State of stress in the conterminous United-States. Journal of Geophysical Research 85, 6113–6156.
Zoback, M.L., Anderson, R.E., Thompson, G.A., 1981. Cainozoic evolution of the state of stress and style of tectonism of the Basin and Range province of the western United States. Philosophical Transactions of the Royal Society London 300, 407–434.